JOURNAL OF THE ROYAL SOCIETY Interface

Magnetic iron compounds in the human brain: a comparison of tumour and hippocampal tissue

Franziska Brem, Ann M Hirt, Michael Winklhofer, Karl Frei, Yasuhiro Yonekawa, Heinz-Gregor Wieser and Jon Dobson

J. R. Soc. Interface 2006 **3**, 833-841
doi: 10.1098/rsif.2006.0133

JOURNAL OF THE ROYAL SOCIETY Interface

J. R. Soc. Interface (2006) **3**, 833–841
doi:10.1098/rsif.2006.0133
Published online 14 June 2006

Magnetic iron compounds in the human brain: a comparison of tumour and hippocampal tissue

Franziska Brem[1], Ann M. Hirt[1,*], Michael Winklhofer[2], Karl Frei[3], Yasuhiro Yonekawa[3], Heinz-Gregor Wieser[4] and Jon Dobson[5]

[1]*Institute of Geophysics, ETH-Hönggerberg, 8093 Zurich, Switzerland*
[2]*Department of Earth and Environmental Science, University of Munich, 80333 München, Germany*
[3]*Department of Neurosurgery, and* [4]*Neurology/EEG, University Hospital Zurich, 8091 Zurich, Switzerland*
[5]*Institute for Science & Technology in Medicine, Keele University, Stoke-on-Trent ST4 7QB, UK*

Iron is a central element in the metabolism of normal and malignant cells. Abnormalities in iron and ferritin expression have been observed in many types of cancer. Interest in characterizing iron compounds in the human brain has increased due to advances in determining a relationship between excess iron accumulation and neurological and neurodegenerative diseases. In this work, four different magnetic methods have been employed to characterize the iron phases and magnetic properties of brain tumour (meningiomas) tissues and non-tumour hippocampal tissues. Four main magnetic components can be distinguished: the diamagnetic matrix, nearly paramagnetic blood, antiferromagnetic ferrihydrite cores of ferritin and ferrimagnetic magnetite and/or maghemite. For the first time, open hysteresis loops have been observed on human brain tissue at room temperature. The hysteresis properties indicate the presence of magnetite and/or maghemite particles that exhibit stable single-domain (SD) behaviour at room temperature. A significantly higher concentration of magnetically ordered magnetite and/or maghemite and a higher estimated concentration of heme iron was found in the meningioma samples. First-order reversal curve diagrams on meningioma tissue further show that the stable SD particles are magnetostatically interacting, implying high-local concentrations (clustering) of these particles in brain tumours. These findings suggest that brain tumour tissue contains an elevated amount of remanent iron oxide phases.

Keywords: brain iron; magnetite; hippocampus; brain ferritin; magnetic properties; meningioma

1. INTRODUCTION

The importance of iron in the human metabolic system and the role of iron in the cell metabolism have been elucidated in numerous studies. A dysfunction in this role has been associated with various benign and malignant disorders (Konemann *et al.* 2005). Abnormalities in iron and ferritin expression have been observed in many types of cancer (Arosio & Levi 2002) and iron overload has been found in association with brain tumours (Kobayashi *et al.* 1997; Mykhaylyk *et al.* 2005). Meningiomas are among the most common occurring types of brain tumours. They evolve from degeneration of cells from the arachnoid membrane and their growth is relatively slow. They are generally considered benign. In this study, magnetic iron phases in meningiomas are characterized.

Three main iron components encountered in the human brain are: (i) haemoglobin-bound iron in the blood, which exhibits nearly paramagnetic behaviour (Mosiniewicz-Szablewska *et al.* 2003), (ii) ferritin, the iron storage protein and (iii) magnetite (Fe_3O_4) and/or maghemite (γ-Fe_2O_3). Ferritin is the primary intracellular iron storage protein and is one of the major proteins of iron metabolism (Arosio & Levi 2002). It consists of a spherical protein shell, 12 nm in diameter, encapsulating a nanoparticle-sized core of antiferromagnetic ferrihydrite ($5Fe_2O_3{\cdot}9H_2O$) with a diameter of up to 8 nm (Chasteen & Harrison1999). Very few magnetic studies have been made on human brain ferritin. A study on the magnetic properties of ferritin from globus pallidus reports that magnetic ordering occurs at 8.5 K (Dubiel *et al.* 1999). Magnetite (Fe_3O_4)

*Author for correspondence (hirt@mag.ig.erdw.ethz.ch).

Received 13 April 2006
Accepted 9 May 2006

was first discovered in the human brain in 1992 (Kirschvink *et al.* 1992), but its physiological origin is still open. The possible role of strongly ferrimagnetic magnetite in neurological and neurodegenerative diseases, such as epilepsy or Alzheimer's disease, has been investigated in several studies (Fuller *et al.* 1995; Schultheiss-Grassi & Dobson 1999; Hautot *et al.* 2003). Independent studies have shown that physiological ferritin cores have a poly-phased structure (Cowley *et al.* 2000; Quintana *et al.* 2000). Using transmission electron microscopy, Quintana *et al.* (2004) found a major amount of magnetite/maghemite-like structures and a minor amount of ferrihydrite structures within isolated molecules of pathological ferritin. Furthermore, using *in-situ* techniques, they identified magnetite-like phases and wüstite-like phases in brain tissue from patients with progressive supranuclear palsy and in hippocampus tissue from patients with Alzheimer's disease (Quintana *et al.* 2006). These findings support the suggestion that ferritin in the human brain might be a precursor for particles of magnetite and/or maghemite with grain sizes that are big enough to carry a remanent magnetization at room temperature (Dobson 2001).

The specific conditions required for the synthesis of magnetite in human brain tissue have not been identified and it is difficult to synthesize under physiological conditions in a laboratory environment. The individual roles of oxygen, phosphorous, the haemoglobin complex and all other elements present in the brain are insufficiently established and too complex to be reproduced. Magnetic methods are highly sensitive for identifying low concentrations of iron phases and therefore are useful in distinguishing between different iron phases in brain tissue. Brem *et al.* (2005*a*) characterized both ferritin and magnetite/maghemite in brain tissue samples by combining different magnetic methods.

In this study, the magnetic properties of 12 meningiomas are magnetically analysed with the goal of contributing to a better understanding of the formation of magnetite and/or maghemite and the preferred conditions for its formation in the human brain. To compare these results to non-tumour human brain tissue, 12 hippocampal tissues were collected from patients with mesial temporal lobe epilepsy (MTLE) after selective amygdalohippocampectomies (Wieser & Yasargil 1982; Wieser 1988).

2. MATERIAL AND METHODS

The 12 meningiomas (WHO Grade I–II) and 12 hippocampal tissues from MTLE patients were resected at the Department of Neurosurgery, University Hospital Zurich and immediately frozen in liquid nitrogen. The two groups are not age-matched and the hippocampal specimens are generally from younger patients (ages ranged from 21 to 59) than the meningiomas (ages ranged from 59 to 80). All procedures were conducted in accordance with the Declaration of Helsinki and approved by the ethics committee of the Canton Zurich. All measurements were made on freshly resected tissues; it was not necessary to use tissues from autopsies. This is important, as it excludes possible effects due to post-mortem chemical changes. Precautions were taken to avoid contaminations, as described in earlier studies (Dobson & Grassi 1996), and all samples were weighed prior to measuring. In the frozen state all samples weighed between 200 and 1200 mg and their dimensions were on the order of 100–800 mm^3. Four types of magnetic measurements were made: (i) acquisition of isothermal remanent magnetization (IRM) and determination of the Wohlfarth-ratio (S); (ii) measurements of induced magnetization (DC susceptibility) as a function of temperature after zero-field cooling (ZFC) and field cooling (FC); (iii) induced magnetization as a function of field (hysteresis loops) at 5 and 300 K; and (iv) first-order reversal curves (FORC) at room temperature.

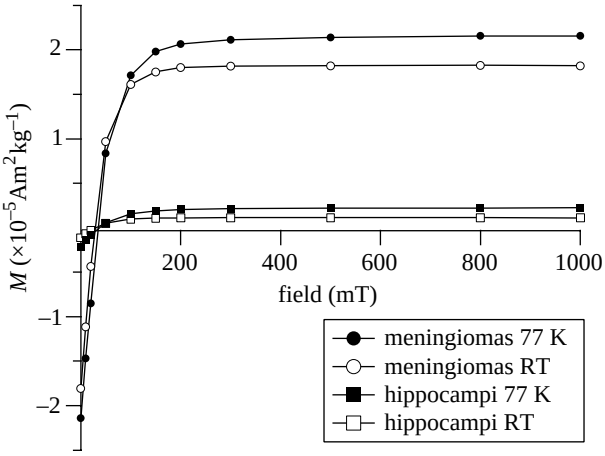

Figure 1. Isothermal remanent magnetization (IRM) acquisition curves at 77 K (filled symbols) and room temperature (open symbols) for meningiomas and hippocampi. All signals are corrected by the weight at 77 K.

The IRM measurements were made on all 24 samples using a 3-axis, 2G Enterprises Superconducting Quantum Interference Device (SQUID) with a sensitivity level of 10^{-11} Am^2. The IRM was acquired in an ASC Scientific Pulse Magnetizer Model IM-10-30, in which the sample was exposed to a pulsed DC field, as follows. First, a pulse of 1 T was applied to the sample and the remanent magnetization was measured. Then, the sample was rotated 180° and progressively increasing fields from 10 mT to 1 T were applied in this opposite direction. This procedure allows for the determination of the coercivity of remanence, B_{cr}. After each magnetizing pulse, the remanent magnetization in the tissue was measured (Brem *et al.* 2005*a*).

All samples were first measured in the frozen state (77 K) and afterwards the tissues were freeze-dried and IRM acquisition was measured at 77 and 300 K. The comparison of the measurements at 77 K on freeze-dried and frozen tissue served as a control for changes during the freeze-drying process. In order to define the Wohlfarth-ratio (Wohlfarth 1958; Cisowski 1981) on freeze-dried tissues, saturation IRM was progressively demagnetized in alternating magnetic fields (AF-demagnetization). This procedure was carried out on six hippocampal tissues and nine meningioma samples.

Induced magnetization was measured as a function of temperature or field on eight samples from each group of tissue using a Quantum Design Magnetic

Table 1. Averaged values for the remanent saturation magnetization (M_{RS}), coercivity of remanence (B_{cr}), the percentage of superparamagnetic particles (% SP) and the Wohlfarth-ratio (S) with ±95% confidence limits (in parentheses) from IRM acquisition at 77 and 300 K (corrected by weight of the sample at 77 K). (The data are for 12 meningiomas and 12 hippocampal tissues, except for the S-values, which are for eight meningioma and eight hippocampi.)

tissue	M_{RS} (77 K)×10^{-5} ($Am^2\,kg^{-1}$)	B_{cr} (77 K) (mT)	M_{RS} (300 K)×10^{-5} ($Am^2\,kg^{-1}$)	B_{cr} (300 K) (mT)	% SP ($M_{RS(77\,K)} - M_{RS(300\,K)}/M_{RS(77\,K)}$)100	S
meningiomas	2.14 (±0.72)	34.5 (±3.6)	1.82 (±0.67)	28.6 (±3.0)	28 (±14)	0.26 (±0.01)
hippocampi	0.22 (±0.04)	34.9 (±4.1)	0.11 (±0.03)	26.2 (±5.1)	37 (±16)	0.32 (±0.04)

Property Measurement System (MPMS) SQUID magnetometer at the Institute for Geosciences, University of Bremen, as well as at the Institute of Rock Magnetism, University of Minnesota and in the Chemistry Department, ETH Zurich. Each of the magnetometers is equipped with an internal field compensation coil and has a residual field of less than 100 μT. The measurements were made on freeze-dried tissue, which was pressed into a straw and fixed by small pinholes without other fixation material.

For the induced magnetization, the samples were initially cooled to 5 K, either in the absence of a magnetic field (ZFC) or in the presence of a weak 50 mT field (FC). At 5 K a magnetic field of 50 mT was applied and the sample was then heated to 300 K, during which the magnetic moment was measured at intervals of no more than 2 K. The magnetization of freeze-dried tissue was also measured as a function of field (hysteresis loop) at 5 K in fields from −5 to 5 T after cooling the samples in zero field. Hysteresis measurements and FORC's at room temperature were made with a Princeton Measurement Alternating Gradient Magnetometer AGM (Model MicroMag 2900) in fields from −0.5 to 0.5 T at the laboratory of the Princeton Measurement Corporation. For these measurements the pressed freeze-dried tissue was cut into round, 2 mm thick slices of diameter 4.5 mm. The slices were mounted on a cleaned silica rod with a very small amount of silicone grease. No further packing material was used. Hysteresis measurements were made on twelve slices from seven meningioma samples and on six slices from three hippocampal samples. The FORC analysis was made on nine slices from seven meningioma samples and on four slices from three hippocampal samples. The alternating gradient head is housed in an acoustic attenuation cabinet to reduce noise due to external vibrations. Before measuring, samples were left mounted overnight so that the sample and holder reached the ambient temperature, which reduced the thermal noise level. The hysteresis curve of the empty silica rod serving as the sample holder in the AGM was measured separately, which has a saturation magnetization M_S of 1.14 (±0.09)×10^{-7} emu.

3. RESULTS

3.1. Isothermal remanent magnetization

The shapes of the isothermal remanent magnetization (IRM) acquisition curves from meningioma and hippocampi are very similar (figure 1). The acquisition shows a rapid increase in low fields and saturation is reached between 200 and 250 mT. Magnetic saturation in fields of this size indicates that hematite (α-Fe_2O_3) is not the magnetic carrier; fine-grained hematite may require fields of 2.5 T or more to produce saturation. The shape of the curves and the saturation fields are indicative of the low-coercivity ferrimagnetic minerals magnetite and/or maghemite (Dunlop & Özdemir 1997). The IRM acquisition curves for both tissue types—and consequently the coercivities of remanence B_{cr}—are similar. The average B_{cr} at 77 K is 34.5 (±3.6) mT for the meningiomas and 34.9 (±4.1) mT for the hippocampi (table 1). At 300 K B_{cr} is lower, where it is 28.6 (±3) mT for the meningiomas and 26.2 (±5.1) mT for the hippocampi (table 1). These B_{cr} values are typical of the coercivities of remanence found in magnetite and/or maghemite (Dunlop & Özdemir 1997). The IRM characteristics and B_{cr} values suggest that the remanent magnetic phases in both types of tissue have predominantly the same magnetic mineralogy. The strength of signal and the remanent saturation magnetization, M_{RS}, however, vary strongly. For meningiomas the average M_{RS} measured at 77 K is 2.14 (±0.72)×10^{-5} $Am^2\,kg^{-1}$, while for the hippocampi the average M_{RS} at 77 K is 0.22(±0.04)×10^{-5} $Am^2\,kg^{-1}$. For both types of samples M_{RS} at

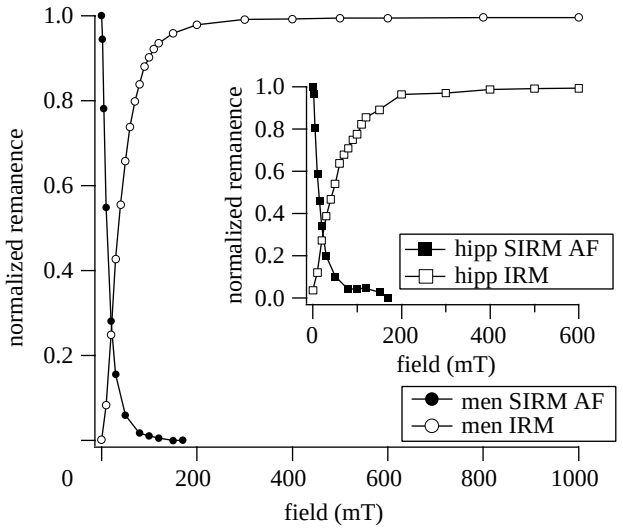

Figure 2. Wohlfarth's ratio (S) from the intersection of the IRM acquisition curve and the AF demagnetization curve of saturation IRM at room temperature for meningiomas (men) and hippocampi (hipp; inset).

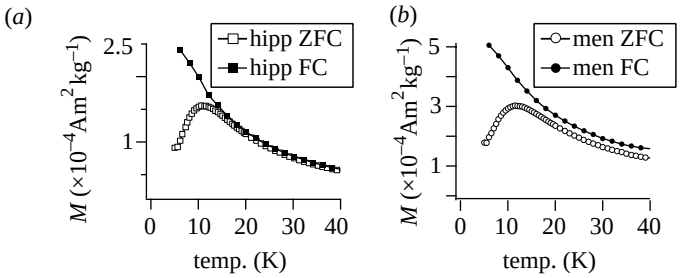

Figure 3. Induced magnetization as a function of temperature after ZFC (open symbols) and FC (filled symbols), measured in a 50 mT field for (*a*) meningiomas (men) and (*b*) hippocampi (hipp).

300 K is less than M_{RS} at 77 K. The difference in M_{RS} is due to magnetic particles, which are superparamagnetic (SP) at room temperature, but whose magnetizations become ordered above 77 K, so that they contribute to the remanent magnetization at low temperature. The average values for the M_{RS} at 300 K are 1.82 ($\pm$0.67)$\times10^{-5}$ Am^2 kg^{-1} for meningiomas and 0.11 ($\pm$0.03)$\times10^{-5}$ Am^2 kg^{-1} for hippocampal tissue (table 1). The percentage of SP particles (% SP) in the temperature range between 77 and 300 K can be expressed by the ratio $(M_{RS}(77\,K)-M_{RS}(300\,K))/(M_{RS}(77\,K))\times100$. The average values are 28 ($\pm$14) % for the meningiomas and (37$\pm$16) % for the hippocampi.

Determination of the Wohlfarth-ratio (S) is shown in figure 2. For non-interacting single-domain (SD) particles with uniaxial anisotropy, the S-ratio is 0.5 (Wohlfarth1958). Lower values are attributed to particle interactions, or to SP or multidomain influences. The average S-ratio for the meningioma samples was 0.26 ($\pm$0.01), while the mean value for the hippocampi was 0.32 ($\pm$0.04). The S-ratios for all measured samples in this study are well below 0.5, which suggests interactions between the particles within the tissue and SP effects.

3.2. Induced magnetization: DC susceptibility as a function of temperature

As brain tissue consists mainly of a diamagnetic fatty matrix with small concentrations of other magnetic components, the method of measuring induced magnetic moment as a function of temperature is very useful (figure 3). The induced magnetization is composed of the diamagnetic signal, a paramagnetic signal from the heme-iron, as well as ferrimagnetic and SP magnetizations. The strength of the diamagnetic contribution, originating from the organic tissue matrix, can be estimated from the temperature-independent magnetization above 250 K. The diamagnetic signal had an average value of -1.62 ($\pm$0.53)$\times10^{-4}$ Am^2 kg^{-1} for the meningiomas and -2.40 ($\pm$0.12)$\times10^{-4}$ Am^2 kg^{-1} for the hippocampi. The magnetic contribution due to the blood has been estimated (Mosiniewicz-Szablewska *et al.* 2003; Brem *et al.* 2005*b*), and can be subtracted from the total magnetic signal. For the meningiomas the average estimated concentration of blood in the samples is about five times higher than in the hippocampi. There are 0.1 ($\pm$0.06) and 0.02 ($\pm$0.009) mg per milligram freeze-dried tissue in the meningioma and hippocampi

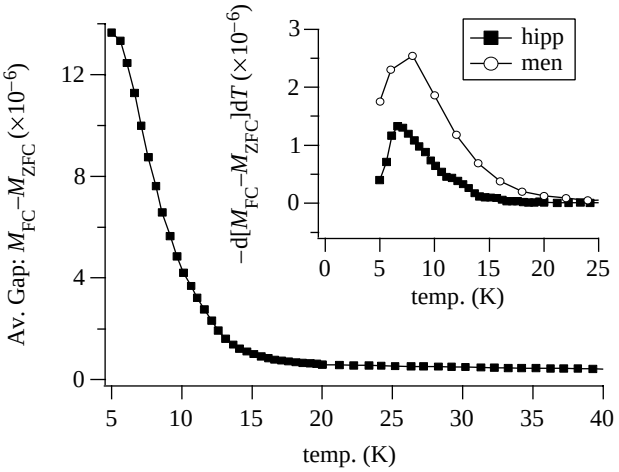

Figure 4. Average displacement between the ZFC magnetization and the FC magnetization for the hippocampi samples, which corresponds to the remanence curve as a function of temperature. The inset shows the derivative of the remanence curve corresponding to the blocking temperature (T_B) distribution as a function of temperature for the hippocampi (hipp) and the meningiomas (men).

samples, respectively. The remaining signal is due to: (i) the SP ferritin, which orders magnetically below 22 K and (ii) an additional remanent (magnetically ordered) phase.

For the characterization of ferritin, the analysis of induced magnetization measurements after both ZFC and FC is the most common method for obtaining information about the blocking behaviour of the protein cores (Makhlouf *et al.* 1997; Dubiel *et al.* 1999). The maximum of the ZFC curve (figure 3*a*,*b*) indicates the average blocking temperature T_B for the SP cores of the protein, which is between 10 and 12 K for all brain samples. No statistically relevant difference of T_B can be seen between hippocampi and meningioma samples.

The existence of another magnetically blocked phase is shown by the behaviour of the ZFC and FC curves. For pure ferritin the curves are expected to bifurcate at approximately 22 K. Above this temperature the curves should superpose completely as all particles become SP (Makhlouf *et al.* 1997). For the meningiomas a distinct displacement can be seen between the ZFC curve and the FC curve (figure 3*b*). For the hippocampi, the displacement is less obvious, but on closer inspection there is no bifurcation of the curves (figure 3*a*). Such a displacement has its origin in the coexistence of a blocked phase (Pardoe & Chua-anusorn 2001), whereby the size of the displacement corresponds to the intensity

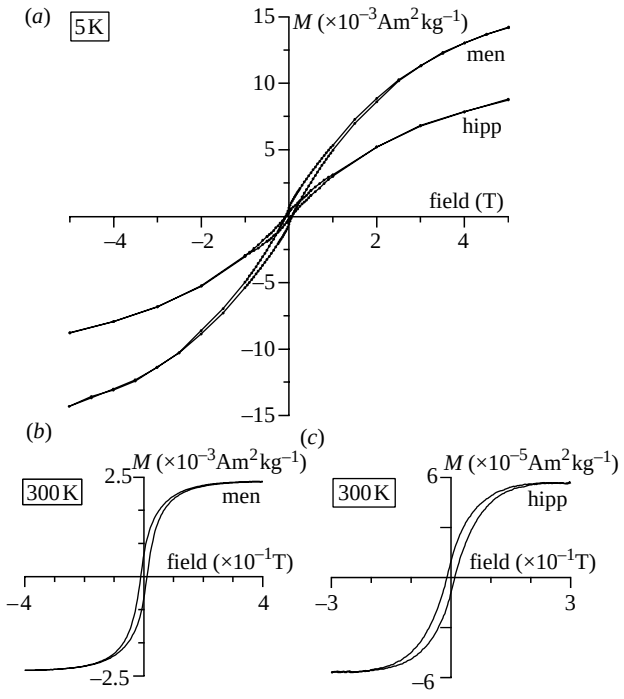

Figure 5. (*a*) Hysteresis at 5 K for the meningioma (men) and hippocampi (hipp), (*b*) hysteresis at 300 K of a meningioma sample (HA1b) and (*c*) hysteresis at 300 K of a hippocampus sample (HH). Note the difference in scale between (*b*) and (*c*). All curves were corrected for linear contributions from the diamagnetic and paramagnetic phases.

of the remanent magnetization of the sample. It thus increases slightly with decreasing temperature between 300 and 20 K, accompanying the further blocking of magnetite and/or maghemite particles. It shows a very steep increase below 20 K (figure 4) due to the superposition of the ferritin ordering. The magnetization difference, $M_{FC}-M_{ZFC}$, between the FC and ZFC curves was obtained by subtraction; it was then differentiated with respect to temperature to obtain the distribution of the blocking temperature T_B of the ferritin cores (figure 4, inset; Hanzlik *et al.* 2000; Mamiya *et al.* 2005).

3.3. Induced magnetization: hysteresis

At 5 K, the hysteresis measurements are dominated by the ferrihydrite cores of ferritin and show an open non-saturating hysteresis up to high fields (figure 5*a*). A slight tendency to wasp-waisting can be seen in several samples; this is due to the effect of the low coercivity phase, magnetite and/or maghemite (Tauxe *et al.* 1996). The coercive force B_c averages 23 ($\pm$10) and 34 ($\pm$10) mT for meningiomas and hippocampi, respectively (table 2). The remanent magnetizations M_{RS} average 3.9 ($\pm$2.3)$\times10^{-4}$ Am^2 kg^{-1} for meningiomas and 2.4 ($\pm$0.6)$\times10^{-4}$ Am^2 kg^{-1} for hippocampi.

Hysteresis curves measured on the AGM at 300 K are shown in figure 5*b* (meningioma sample) and figure 5*c* (hippocampus sample). The hysteresis loops at room temperature are open. Until now, open hysteresis loops have only been observed on human tissue at low temperature, e.g. at 150 K (Hautot *et al.* 2003). The room temperature behaviour of ferritin is completely SP and does not contribute to the hysteresis loop, which is due to the ferrimagnetic component. B_c is 10.5 mT for the meningioma sample, HA1b and 9.8 mT for the hippocampus sample, HH (where the sample labelling identifies patients by their initials). The remanent saturation magnetization M_{RS} and the induced saturation magnetization M_S for the meningioma HA1b are 5.48×10^{-4} Am^2 kg^{-1} and 2.38×10^{-3} Am^2 kg^{-1}, respectively. The ratios M_{RS}/M_S and B_{cr}/B_c are 0.23 and 1.93, respectively. For the hippocampus sample HH, M_{RS} is 9.38×10^{-6} Am^2 kg^{-1} and M_S is 5.67×10^{-5} Am^2 kg^{-1}. The M_{RS}/M_S ratio is 0.17 and the B_{cr}/B_c ratio is 3.5. The average B_c is 8.4 ($\pm$1.8) mT for the meningiomas and 7.7 ($\pm$1.4) mT for the hippocampi, while the average M_{RS} is 1.42 ($\pm$0.99)$\times10^{-4}$ Am^2 kg^{-1} for the meningiomas and 0.07 ($\pm$0.007)$\times10^{-4}$ Am^2 kg^{-1} for the hippocampi (table 2). These average values cannot be directly compared to the values of the IRM acquisition, because of the different normalization. However, the values are in good agreement with each other.

3.4. First-order reversal curves

The FORC data were obtained from slices of several meningioma and hippocampi samples. The variation of magnetization between different tissues is large, as was the case for the IRM acquisition and the hysteresis measurements. Therefore, different smoothing factors were necessary, depending on the weakness of the sample signal. In figure 6*a–d*, FORC diagrams of four different samples (three meningiomas and one hippocampus) are compared. The parameter B_c corresponds to the coercivity distribution and the parameter B_b corresponds to the distribution of interaction fields. All samples show a pronounced vertical spread along B_b and an intensification of signal around the origin due to SP behaviour of the ferrimagnetic phase; this is due to thermal relaxation that shifts the B_c distribution towards lower values (Pike *et al.* 2001). The FORC diagram of the strongest sample HA1a, a meningioma, shows a maximum in the microcoercivity distribution (along B_c axis) at a B_c of 14 mT (figure 6*a*). A second weaker increase can be seen towards $B_c=0$. In a second slice, HA1b (meningioma), the local maximum around $B_c=14$ mT is repeatable (figure 6*b*), but the strength of signal decreases slightly compared to HA1a and the coercivity distribution around the origin is enhanced. In figure 6*c* (HM2b, meningioma) the overall strength of signal becomes very weak, but a small local maximum in the coercivity distribution at slightly lower B_c (11 mT) is still observed. The distinct local maximum in coercivity distribution completely disappears in the diagram in figure 6*d*. The signal in HH is extremely weak and the FORC diagram is strongly dominated by the SP contribution around the origin.

4. DISCUSSION

The results of these magnetic measurements illustrate that human brain tissue contains four major magnetic components: diamagnetic tissue, nearly paramagnetic blood, antiferromagnetic ferrihydrite cores of ferritin

Table 2. Averaged values for the blood content, the average blocking temperature (T_B), coercive force (B_c) and the remanent saturation magnetization (M_{RS}) with ±95% confidence limits (in parentheses) from induced magnetization measurements as a function of temperature and hysteresis measurements at 5 and 300 K (corrected by freeze-dried weight of the sample). (The data are for eight meningiomas and eight hippocampal tissues, except for the B_c (300 K) and M_{RS} (300 K), which are for 12 meningioma slices and six hippocampi slices.)

tissue	blood content (mg mg^{-1} tissue$_{fd}$)	T_B (K)	B_c (5 K) (mT)	M_{RS} (5 K)×10^{-4} (Am^2 kg^{-1})	B_c (300 K) (mT)	M_{RS} (300 K)×10^{-4} (Am^2 kg^{-1})
meningiomas	0.10 (±0.060)	11.7 (±0.4)	23 (±10)	3.9 (±2.3)	8.4 (±1.8)	1.42 (±0.990)
hippocampi	0.02 (±0.009)	10.9 (±0.4)	34 (±10)	2.4 (±0.6)	7.7 (±1.4)	0.07 (±0.007)

and ferrimagnetic magnetite and/or maghemite. The magnetic detection of these components is in good agreement with reported results from X-ray absorption spectroscopy on brain tissue (Collingwood *et al.* 2005; Mikhaylova *et al.* 2005). Meningioma and hippocampal samples show equivalent diamagnetic properties. Measurements of induced magnetization as a function of field and temperature show that magnetic behaviour of ferritin is approximately the same for both types of tissue. IRM acquisition shows that meningiomas contain approximately ten times more ferrimagnetic particles than the hippocampi. This difference is also expressed in a displacement between the ZFC and FC curves in the induced magnetization and in wasp-waisted hysteresis curves at 5 K. The open hysteresis loops and FORC analysis at room temperature are compatible with SD behaviour in magnetite and/or maghemite, while smaller, SP particles would reveal closed loops e.g. (Morales *et al.* 1999). Magneto-mineralogical studies in fine-grained magnetite have shown that the transition from SP to SD behaviour occurs at grain sizes around 25–30 nm (Dunlop & Özdemir 1997). The hysteresis and FORC analyses show that, in addition to the SD-component, there is also a SP component from smaller grains. The SP signal dominates some samples, especially the weaker hippocampi. *S*-ratios were all below 0.5 for both tissue types, which suggests that the ferrimagnetic grains are interacting. FORC diagrams further suggest that these particles are not homogeneously distributed throughout the tissue, but cluster in distinct areas. To assess the role of magnetostatic interactions in our samples, it is helpful to compare the FORC diagrams for the meningiomas with FORC diagrams for a synthetic reference sample, a concentrated SD magnetite powder sample (Pan *et al.* 2005). The half-width fields in our meningioma samples range from 6 to 10 mT, measured along vertical sections through the isolated peak of the FORC distribution, which corresponds well with the 8.2 mT for the synthetic SD magnetite powder sample. This similarity strongly suggests that the SD particles in the meningioma samples form local clusters rather than occurring isolated. In the case of the hippocampus sample it is more difficult to specify the coercivity value through which to draw a profile yielding the half-width field because the FORC distribution does not show an isolated maximum any more but increases monotonously towards the left margin of the diagram. At 10 mT, roughly where the peaks of the FORC distributions for the other samples are located, we obtain a half-width of 14 mT.

The saturation magnetization deduced from the hysteresis loop at room temperature of the meningiomas exceeds M_{RS} of the hippocampi, expected from the observed difference in the IRM measurements. In the study by Kirschvink *et al.* (1992), the magnetite concentrations in meninges, which were calculated from saturation IRM, were an order of magnitude higher than those from the cerebrum and the cerebellum. Furthermore, the magnetite/maghemite concentrations measured in this study are comparable to the values in meningioma measured by Kobayashi *et al.* (1997). It is known that brain iron burden increases with aging (Burdo & Connor 2003; Bartzokis *et al.* 2004), which theoretically could influence our results. However, no correlation of magnetite and/or maghemite content with age was found in either type of tissue. In addition, a comparison of results from the two youngest meningioma patients with the results from the oldest hippocampi patients revealed the same statistically significant difference as for the average values from all patients.

The average estimated blood content in the meningiomas is higher than in the hippocampi. The relation between blood supply within the tissue and the formation of magnetite and/or maghemite is unknown. However, the broad particle size distribution, shown by the difference of M_{RS} in the IRM acquisition, the increasing displacement in the ZFC-FC measurements, the ratios M_{RS}/M_S and B_{cr}/B_c in conjunction with the different FORC diagrams suggest that particle growth starts at nanometric size and different growth states are detected within all tissue samples. In the hippocampi the sizes are smaller, while in the meningioma the conditions may be more favourable for growth of larger particles. Such a process would support the idea that ferritin behaves as a precursor for magnetite and/or maghemite growth (Dobson 2001; Quintana *et al.* 2004). In the present study, however, it has been shown that the formation of strongly ferrimagnetic particles is favoured in the meningiomas compared to hippocampal tissue.

5. CONCLUSIONS

The magnetic methods described in this study show that human meningiomal brain tumour tissues contain an order of magnitude higher concentration of ferrimagnetic particles than non-tumour hippocampi. Although these tumours are well vascularized, it is not yet known whether blood supply plays a role in this

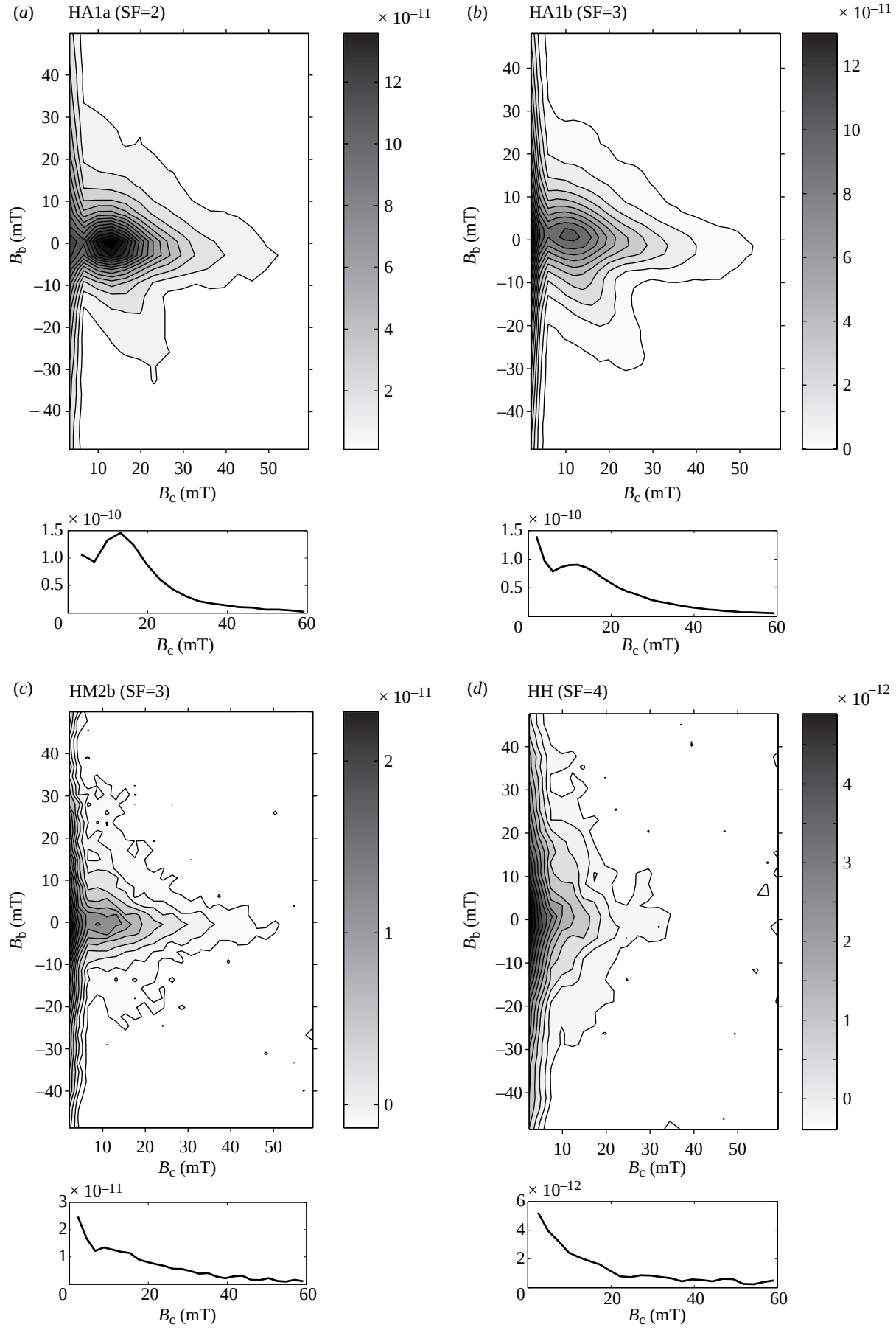

Figure 6. First-order reversal curves (FORC) measured at room temperature for four different tissue samples: (*a*) meningioma HA1a, (*b*) meningioma HA1b, (*c*) meningioma (HM2b) and (*d*) hippocampus HH. The section below each figure presents the profile along the B_c-axis.

higher concentration. Iron distribution in the brain is heterogeneous. However, the formation rate of ferrimagnetic magnetite and/or maghemite appears to be higher in the tumour tissue. FORC diagrams provide insight into room-temperature coercivity distributions in human brain tissue and can be used to assess the role of magnetostatic interactions as proxy of magnetic particle concentration. We observed a pronounced vertical spread in the FORC diagram implying high local concentrations of magnetic remanence carriers. This information may provide insights into differences in iron metabolism in tumour versus non-tumour tissue. Our magnetic results demonstrate that these methods, in combination with medical research, can lead to a better understanding of iron physiology in the human brain.

We thank the Institute for Geosciences at the University of Bremen, the Institute of Rock Magnetism at the University of Minneapolis and the Chemistry Department at ETH Zurich, especially Dr Thomas Frederichs, Dr Mike Jackson, Peat Solheid and Alois Weber for the use of the MPMS and very helpful discussions. We acknowledge W. Lowrie and three anonymous reviewers for their helpful comments. We also thank the Princeton Measurement Corporation (PMC) for the use of their AGFM and their help in enhancing its sensitivity. J.D. gratefully acknowledges the support of a Royal Society/Wolfson Foundation Research Merit Award. F.B. and A.M.H. acknowledge support from ETH project 0-20118-03. This is ETH contribution number 1453.

REFERENCES

Arosio, P. & Levi, S. 2002 Ferritin, iron homeostasis, and oxidative damage. *Free Radic. Biol. Med.* **33**, 457–463. (doi:10.1016/S0891-5849(02)00842-0)

Bartzokis, G., Tishler, T. A., Shin, I. S., Lu, P. H. & Cummings, J. L. 2004 Brain ferritin iron as a risk factor for age at onset in neurodegenerative diseases. *Ann. N Y Acad. Sci.* **1012**, 224–236. (doi:10.1196/annals.1306.019)

Brem, F., Hirt, A. M., Simon, C., Wieser, H. G. & Dobson, J. 2005*a* Characterization of iron compounds in tumour tissue from temporal lobe epilepsy patients using low temperature magnetic methods. *Biometals* **18**, 191–197. (doi:10.1007/s10534-004-6253-y)

Brem, F., Hirt, A. M., Simon, C., Wieser, H. G. & Dobson, J. 2005*b* Low temperature magnetic analysis in the identification of iron compounds from human brain tumor tissue. *J. Phys. Conf. Ser.* **17**, 61–64. (doi:10.1088/1742-6596/17/1/010)

Burdo, J. R. & Connor, J. R. 2003 Brain iron uptake and homeostatic mechanisms: an overview. *Biometals* **16**, 63–75. (doi:10.1023/A:1020718718550)

Chasteen, N. D. & Harrison, P. M. 1999 Mineralization in ferritin: an efficient means of iron storage. *J. Struct. Biol.* **126**, 182–194. (doi:10.1006/jsbi.1999.4118)

Cisowski, S. 1981 Interacting vs. non-interacting single domain behavior in natural and synthetic samples. *Phys. Earth Planet. Int.* **26**, 56–62. (doi:10.1016/0031-9201(81)90097-2)

Collingwood, J. F., Mikhaylova, A., Davidson, M., Batich, C., Streit, W. J., Terry, J. & Dobson, J. 2005 *In situ* characterization and mapping of iron compounds in Alzheimer's disease tissue. *J. Alzheimers Dis.* **7**, 267–272.

Cowley, J. M., Janney, D. E., Gerkin, R. C. & Buseck, P. R. 2000 The structure of ferritin cores determined by electron nanodiffraction. *J. Struct. Biol.* **131**, 210–216. (doi:10.1006/jsbi.2000.4292)

Dobson, J. 2001 Nanoscale biogenic iron oxides and neurodegenerative disease. *FEBS Lett.* **496**, 1–5. (doi:10.1016/S0014-5793(01)02386-9)

Dobson, J. & Grassi, P. 1996 Magnetic properties of human hippocampal tissue—evaluation of artefact and contamination sources. *Brain Res. Bull.* **39**, 255–259. (doi:10.1016/0361-9230(95)02132-9)

Dubiel, S. M., Zablotna-Rypien, B., Mackey, J. B. & Williams, J. M. 1999 Magnetic properties of human liver and brain ferritin. *Eur. Biophys. J. Biophys. Lett.* **28**, 263–267.

Dunlop, D. J. & Özdemir, Ö. 1997 *Rock magnetism, fundamentals and frontiers*, 1st edn. Cambridge, UK: Cambridge University Press.

Fuller, M., Dobson, J., Wieser, H. G. & Moser, S. 1995 On the sensitivity of the human brain to magnetic-fields—evocation of epileptiform activity. *Brain Res. Bull.* **36**, 155–159. (doi:10.1016/0361-9230(94)00183-2)

Hanzlik, M., Heunemann, C., Holtkamp-Rotzler, E., Winklhofer, M., Petersen, N. & Fleissner, G. 2000 Superparamagnetic magnetite in the upper beak tissue of homing pigeons. *Biometals* **13**, 325–331. (doi:10.1023/A:1009214526685)

Hautot, D., Pankhurst, Q. A., Khan, N. & Dobson, J. 2003 Preliminary evaluation of nanoscale biogenic magnetite in Alzheimer's disease brain tissue. *Proc. R. Soc. B* **270** (Suppl. 1), S62–S64. (doi:10.1098/rsbl.2003.0012)

Kirschvink, J. L., Kobayashi-Kirschvink, A. & Woodford, B. J. 1992 Magnetite biomineralization in the human brain. *Proc. Natl Acad. Sci. USA* **89**, 7683–7687. (doi:10.1073/pnas.89.16.7683)

Kobayashi, A. K., Yamamoto, N. & Kirschvink, J. L. 1997 Studies of inorganic crystals in biological tissue: magnetite in human tumors. *J. Jap. Soc. Powder Powder Metall.* **44**, 294–300.

Konemann, S., Bolling, T., Matzkies, F., Willich, N., Kisters, K. & Micke, O. 2005 Iron and iron-related parameters in oncology. *Trace Elem. Electrolytes* **22**, 142–149.

Makhlouf, S. A., Parker, F. T. & Berkowitz, A. E. 1997 Magnetic hysteresis anomalies in ferritin. *Phys. Rev. B* **55**, R14717–R14720. (doi:10.1103/PhysRevB.55.R14717)

Mamiya, H., Ohnuma, A., Nakatani, I. & Furubayashim, T. 2005 Extraction of blocking temperature distribution from zero-field-cooled and field-cooled magnetization curves. *IEEE Trans. Magn.* **41**, 3394–3396. (doi:10.1109/TMAG.2005.855205)

Mikhaylova, A., Davidson, M., Toastmann, H., Channell, J. E. T., Guyodo, Y., Batich, C. & Dobson, J. 2005 Detection, identification and mapping of iron anomalies in brain tissue using X-ray absorption spectroscopy. *J. R. Soc. Interface* **2**, 33–37. (doi:10.1098/rsif.2004.0011)

Morales, M. P., Veintemillas-Verdaguer, S., Montero, M. I., Serna, C. J., Roig, A., Casas, L., Martinez, B. & Sandiumenge, F. 1999 Surface and internal spin canting in gamma-Fe2O3 nanoparticles. *Chem. Mat.* **11**, 3058–3064. (doi:10.1021/cm991018f)

Mosiniewicz-Szablewska, E., Slawska-Waniewska, A., Swiatek, K., Nedelko, N., Galazka-Friedman, J. & Friedman, A. 2003 Electron paramagnetic resonance studies of human liver tissues. *Appl. Magn. Reson.* **24**, 429–435.

Mykhaylyk, O., Dudchenko, N., Cherchenko, A., Rozumenko, V. & Zozulya, Y. 2005 Dysregulation of non-heme iron metabolism in glial brain tumors. *Med. Princ. Pract.* **14**, 221–229. (doi:10.1159/000085739)

Pan, Y. X., Petersen, N., Winklhofer, M., Davila, A. F., Liu, Q. S., Frederichs, T., Hanzlik, M. & Zhu, R. X. 2005 Rock

magnetic properties of uncultured magnetotactic bacteria. *Earth Planet. Sci. Lett.* **237**, 311–325. (doi:10.1016/j.epsl.2005.06.029)

Pardoe, H., Chua-anusorn, W., St Pierre, T. G. & Dobson, J. 2001 Structural and magnetic properties of nanoscale iron oxide particles synthesized in the presence of dextran or polyvinyl alcohol. *J. Magn. Magn. Mater.* **225**, 41–46. (doi:10.1016/S0304-8853(00)01226-9)

Pike, C. R., Roberts, A. P. & Verosub, K. L. 2001 First-order reversal curve diagrams and thermal relaxation effects in magnetic particles. *Geophys. J. Int.* **145**, 721–730. (doi:10.1046/j.0956-540x.2001.01419.x)

Quintana, C., Lancin, M., Marhic, C., Perez, M., Martin-Benito, J., Avila, J. & Carrascosa, J. L. 2000 Initial studies with high resolution TEM and electron energy loss spectroscopy studies of ferritin cores extracted from brains of patients with progressive supranuclear palsy and Alzheimer disease. *Cell. Mol. Biol.* **46**, 807–820.

Quintana, C., Cowley, J. M. & Marhic, C. 2004 Electron nanodiffraction and high-resolution electron microscopy studies of the structure and composition of physiological and pathological ferritin. *J. Struct. Biol.* **147**, 166–178. (doi:10.1016/j.jsb.2004.03.001)

Quintana, C., Bellefqih, S., Laval, J. Y., Guerquin-Kern, J. L., Wu, T. D., Avila, J., Ferrer, I., Arranz, R. & Patino, C. 2006 Study of the localization of iron, ferritin, and hemosiderin in Alzheimer's disease hippocampus by analytical microscopy at the subcellular level. *J. Struct. Biol.* **153**, 42–54. (doi:10.1016/j.jsb.2005.11.001)

Schultheiss-Grassi, P. P. & Dobson, J. 1999 Magnetic analysis of human brain tissue. *Biometals* **12**, 67–72. (doi:10.1023/A:1009271111083)

Tauxe, L., Mullender, T. A. T. & Pick, T. 1996 Potbellies, wasp-waists, and superparamagnetism in magnetic hysteresis. *J. Geophys. Res. B* **101**, 571–583. (doi:10.1029/95JB03041)

Wieser, H. G. 1988 Selective amygdalo-hippocampectomy for temporal-lobe epilepsy. *Epilepsia* **29**, 100–113.

Wieser, H. G. & Yasargil, M. G. 1982 Selective amygdalo-hippocampectomy as a surgical-treatment of mesiobasal limbic epilepsy. *Surg. Neurol.* **17**, 445–457.

Wohlfarth, E. P. 1958 Relations between different modes of acquisition of the remanent magnetization of ferromagnetic particles. *J. Appl. Phys.* **29**, 595–596. (doi:10.1063/1.1723232)